Buckling Strength of Imperfect Spherical Caps—Some Remarks

J. Blachut* and G. D. Galletly†
University of Liverpool, Liverpool, United Kingdom

Introduction

THERE have been many investigations over the past 30–40 yr dealing with the effects of geometric imperfections on the buckling strength of various types of shell. Externally pressurized spherical caps/hemispheres are shells for which small initial deviations in the shape of the shell can decrease the buckling pressure significantly. This is the case for both elastic and elastic-plastic material properties. Various arbitrary imperfections in shape have been postulated and their influence assessed by analytical and numerical approaches. Some experimental verification has also been undertaken (see Refs. 1–3 for a comprehensive reference list). Among axisymmetric imperfections, the following three types have been studied: 1) an increased-radius local "flat" spot; 2) a smooth inward dimple; and 3) the Legendre polynomial.

Use of lower-bound curves, based on 1) an increased-radius "flat" spot located at the apex of the shell and 2) on the Legendre polynomial type imperfection, were presented in Ref. 3 for elastic and elastic-plastic clamped hemispheres subjected to external pressure.

The main aim of this Note is to examine the influence of a smooth inward dimple and an increased-radius "flat" spot imperfection on the buckling strength of a spherical cap. The present results differ from those published in Refs. 4 and 5. However, the latter results were not based on the lower-bound curve concept.

Geometry and Imperfection Shapes in Spherical Caps

Let us consider an externally pressurized, clamped spherical cap of radius R, thickness t, and semiangle $\alpha = 16.26$ deg (Fig. 1b). The shape of the smooth dimple type imperfection is assumed as

$$w = (\delta_o/t)\,(1-x^2)^3 \tag{1}$$

where δ_o is the amplitude of the imperfection at the apex, $x = s/s_{imp}$, and s_{imp} is the meridional extent of the imperfection. Calculations show that the reduction in the buckling pressure depends on s_{imp}.[3,9] Several profiles of the radial deviation w, defined by Eq. (1), are shown in Fig. 1a for $\delta_o/t = 1.0$ and $s_{imp} = 25\%$, 50%, 75%, and 100% of the total meridional length. The geometry of the increased-radius "flat" spot located at the apex is shown in Fig. 1c.

Comparison of Bifurcation/Snap-Through Pressures for Some Perfect Spherical Caps

Prior to carrying out a numerical investigation of imperfection sensitivity, a comparison was made of the theoretical predictions of bifurcation/snap-through buckling pressures for some perfect caps using the ABAQUS, BOSOR 5, and FASOR-EP programs.[6-8] Three values of λ were considered, i.e., $\lambda = 5$, 7.5, and 10, where $\lambda = 2[3(1-\nu^2)]^{0.25}(H/t)^{0.5}$, and ν is the Poisson's ratio. H and t are the height and the thickness of the spherical cap, respectively (see Fig. 1b).

Received May 22, 1989; revision received July 14, 1989.

*University Research Fellow, Department of Mechanical Engineering.

†Professor of Applied Mechanics, Department of Mechanical Engineering.

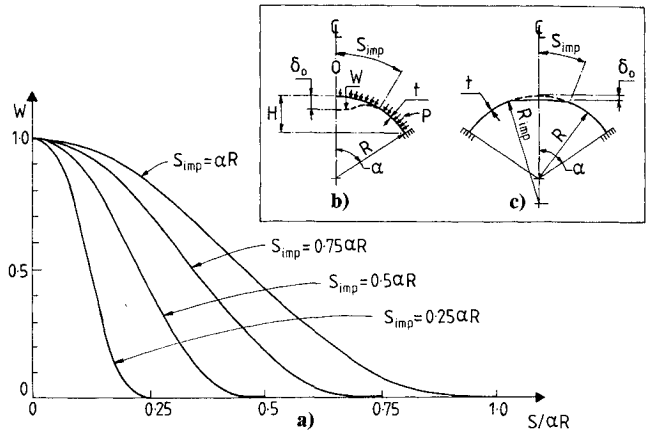

Fig. 1 Four different profiles of a smooth inward dimple (Fig. 1a). Geometry of a cap with inward dimple (Fig. 1b) and an increased-radius flat spot (Fig. 1c) imperfection.

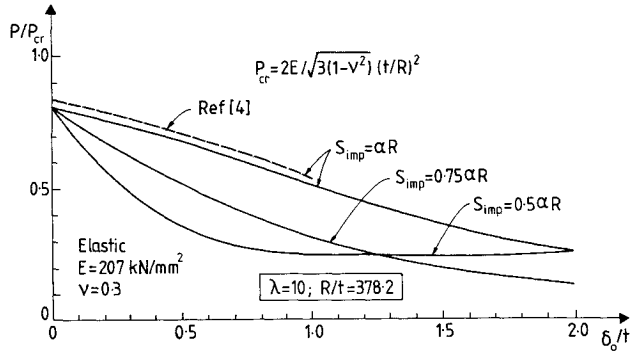

Fig. 2 Influence of the extent of an inward dimple imperfection on the buckling pressure.

Table 1 gives the elastic and elastic-plastic buckling pressures of the steel caps under consideration. The results obtained for the axisymmetric buckling pressures using the ABAQUS, BOSOR 5, and FASOR-EP codes were very similar. The bifurcation buckling pressures, however, were consistently below those of Ref. 4, which predicted snap-through; for the elastic spherical cap having $\lambda = 7.5$, the bifurcation buckling pressure was as much as 35% below the snap-through pressure.

Lower-Bound Curves for Imperfect Spherical Caps($\lambda = 6$ and $\lambda = 10$)

The BOSOR 5 program, based on Novozhilov-Sander's nonlinear shell theory and the finite-difference energy method, was used in the past by the authors to analyze the response of externally pressurized hemispheres to geometrical imperfections.[3] As a natural extension, it was decided to use it again to examine the buckling resistance of some imperfect spherical caps. The imperfection shape considered in this section was that of a smooth inward dimple as defined by Eq. (1). The initial computations were performed for $\lambda = 10$ and elastic material. The results obtained, for various values of the imperfect zone along the meridian, are shown in Fig. 2. For a given δ_o/t, the calculations show that the reduction in the buckling strength varies with the meridional extent of the imperfection. They also show that the lowest collapse pressures do not necessarily correspond to imperfections which cover the whole cap (i.e., $s_{imp} = \alpha R$).

Using a finer variation in s_{imp} in Fig. 2 produces many curves. Then, drawing the envelope to all these curves gives the curve shown in Fig. 3 (this is called a lower-bound curve—see Figs. 15 and 16 in Ref. 3). A similar sensitivity to imperfections was also obtained for spherical caps which had elastic-plastic material properties. As shown in Fig. 3, the rel-

Table 1 Comparison of bifurcation/snap-through dimensionless buckling pressures for steel caps[a]

		Elastic						Elastic-Plastic					
		Snap-through				Bifurcation		Snap-through				Bifurcation	
λ	R/t	Ref. 4	BOSOR	FASOR	ABAQUS	BOSOR	FASOR	Ref. 4	BOSOR	FASOR	ABAQUS	BOSOR	FASOR
5	96.15	0.64	0.62	0.65	0.63	——	——	0.31	0.31	0.32	0.31	——	——
7.5	212.77	1.01	1.08	1.10	1.09	0.75 (3)	0.76 (3)	0.58	0.59	0.59	0.59	0.55 (4)	0.54 (4)
10	378.22	0.85	0.81	0.85	0.81	0.77 (5)	0.77 (5)	0.83	0.80	0.82	0.80	0.76 (5)	0.76 (5)

[a]The normalization factor $p_{cr}^* = 2E/[3(1-\nu^2)]^{0.5}\,(t/R)^2$. Material properties are the same as in Refs. 4 and 5, i.e., $E = 207$ kN/mm^2, $\sigma_{yp} = 207$ N/mm^2, and $E_t = 0.1\,E$.

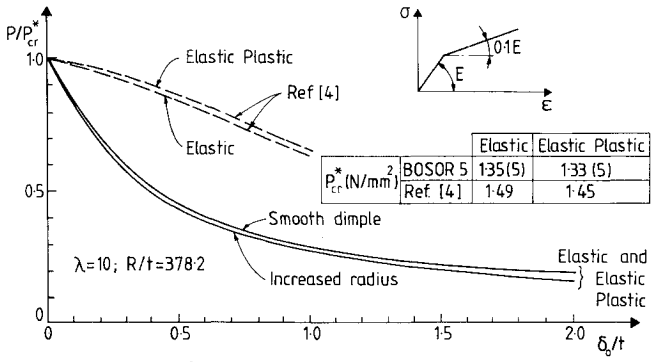

Fig. 3 Lower-bound curves for the elastic/elastic-plastic buckling pressures of imperfect spherical caps. Note the erosion of the buckling pressure by both the dimple and the increased-radius imperfections. Results from Ref. 4 are also depicted.

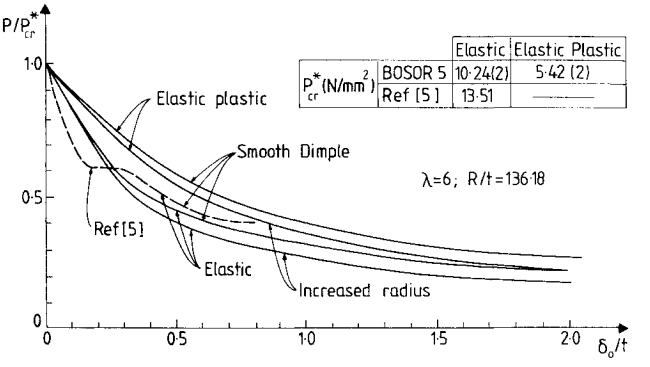

Fig. 4 Influence of both dimple and flat-spot imperfections on the buckling strength (lower bound). Results from Ref. 5 are also depicted—note $p_{cr}^* = 13.51$ N/mm^2 in this case.

ative reductions in the elastic and the elastic-plastic buckling pressures are similar in the range $0 \le \delta_o/t \le 2.0$. Also, as shown in Fig. 3, there is a big difference between the results of Ref. 4, based on $s_{imp} = \alpha R$, and the lower-bound curve obtained for variable s_{imp}.

A related problem was examined in Ref. 5 for an elastic spherical cap with $\lambda = 6$ where, once again, $s_{imp} = \alpha R$ was assumed. The smooth inward dimple imperfection (in the form of Eq. (1) with $s_{imp} = \alpha R$) reduced the buckling pressure, as shown in Fig. 4, for $0 < \delta_o/t \le 0.8$. The buckling pressures decrease as the amplitude δ_o/t increases but, for the larger amplitudes of δ_o/t, the decrease in buckling strength seems to diminish. The buckling pressures of the above-mentioned Ref. 5 are only directly comparable with the results of this Note if they are multiplied by the factor 13.51/10.24 (due to the pressures in Ref. 5 being normalized with respect to the pressure corresponding to the symmetric mode of failure, i.e., 13.51 N/mm^2). When this factor is taken into account, a comparison of the results shows, once again, that the reduction in the buckling strength, based on $s_{imp} = \alpha R$, is less than that based on the lower-bound approach. As the extent and the amplitude of imperfections in practice are not usually known, one should presumably design for the worst situation. The assumption that $s_{imp} = \alpha R$ might not give a safe assessment of the buckling pressure.

Figure 4 also shows a decrease in the buckling pressure as a function of δ_o/t for elastic-plastic material properties. Spherical caps having $\lambda = 6$ are slightly less sensitive to axisymmetric imperfections in the elastic-plastic range then are similar spherical caps in the elastic range.

The Smooth Dimple vs the Increased-Radius Imperfection

The lower-bound curves described above, for spherical caps with $\lambda = 6$ and $\lambda = 10$, were obtained assuming an axisymmetric imperfection defined by Eq. (1). A similar lower-bound curve can also be calculated for the increased-radius axisymmetric "flat" spot. The numerical results are superimposed in Figs. 3 and 4 for $\lambda = 6$ and $\lambda = 10$, respectively. As may be seen, there is very little difference between the results corresponding to these two ways of modeling the geometrical deviations. For both of the spherical caps considered here ($\lambda = 6$ and $\lambda = 10$), the increased-radius imperfections gave a slightly larger reduction in the buckling pressures.

Conclusions

Two spherical cap geometries were considered in this Note. For each geometry, two types of initial imperfection were examined for both elastic and elastic-plastic material properties. A search for the lower-bound curve was carried out for both types of imperfection.

For steel caps having $\lambda = 6$ and $\lambda = 10$, the present numerical results (based on BOSOR 5) showed that there was only a relatively small difference between the buckling pressures corresponding to a smooth inward dimple and those for an increased-radius "flat" spot imperfection.

The assumed material properties (i.e., steel with linear strain hardening—see Table 1 and Fig. 3) influence the buckling pressures for $\lambda = 6$, where a smaller sensitivity to imperfections was found for elastic-plastic buckling than for elastic buckling.

The difference in buckling pressures was much less for $\lambda = 10$. The same trend in the buckling strength vs imperfection amplitude was observed in Ref. 3 for elastic-perfectly-plastic material (steel and aluminum). However, it seems that there has not been any thorough quantitative assessment of the influence of strain hardening on the buckling strength of imperfect spherical caps.

There was also a considerable disparity between the buckling strengths based on the lower-bound concept discussed herein and those of Refs. 4 and 5. In essence, the results of Refs. 4 and 5 are based on the axisymmetric imperfection being spread over the whole length of a meridian. This does not necessarily represent the worst case from the practical point of view.

References

[1]Kollár, L. and Dulácska, E., *Buckling of Shells for Engineers*, Wiley, New York, 1984.

[2]Bushnell, D., *Computerized Buckling Analysis of Shells*, Martinus Nijhoff Publishers, The Netherlands, 1985.

[3]Galletly, G. D., Blachut, J., and Krużelecki, J., "Plastic Buckling of Imperfect Hemispherical Shells Subjected to External Pressure,"

Proceedings of the Institute of Mechanical Engineers, Vol. 201, No. C3, pp. 153-170, 1987.

[4]Kao, R., "Large Deformation Elastic-Plastic Buckling Analysis of Spherical Caps with Initial Imperfections," *Computers and Structures,* Vol. 11, 1980, pp. 609-619.

[5]Yang, T. Y. and Liaw, D. G., "Elastic-Plastic Dynamic Buckling of Thin-Shell Finite Elements with Asymmetric Imperfections," *AIAA Journal,* Vol. 26, No. 4, 1988, pp. 479-486.

[6]Hibbitt, H. D., Karlsson, B. I., and Sorensen, E. P., *ABAQUS—User Manual,* Version 4.5, HKS, Inc., RI, 1984.

[7]Bushnell, D., "BOSOR 5—Program for Buckling of an Elastic-Plastic Complex Shells of Revolution Including Large Deflections and Creep," *Computers and Structures,* Vol. 6, 1976, pp. 221-239.

[8]"FASOR—A Program for Stress, Buckling, and Vibration of Shells of Revolution," Advances in Engineering Software, Vol. 3, 1981, pp. 155-162.

[9]Bushnell, D., "Nonlinear Axisymmetric Behavior of Shells of Revolution," *AIAA Journal,* Vol. 5, No. 3, 1967, pp. 432-439.

Effect of Thermomechanical Coupling on the Response of Elastic Solids

A. M. Amin* and R. L. Sierakowski†
Ohio State University, Columbus, Ohio

Introduction

THIS Note treats a condition that arises when a solid body is subjected to a highly transient heating or cooling, sometimes referred to as "thermal shock" exposure. The phenomenon is of greatest significance for completely elastic or "brittle" materials, where it may produce material fracture. Many high temperature materials such as ceramics and intermetallics fall into this category.

Thermal response of elastic solids is always accompanied by two important phenomena; the coupling between the thermal and mechanical energy and the inertia effects. A few problems have been solved to show their effects on the stress and the temperature distributions of isotropic solids subjected to thermal loads. However, one can investigate the reasonableness of neglecting these effects by comparing exact and approximate solutions to a specific problem. Some classical discussions of thermomechanical coupling include Mindlin and Goodman,[1] Boley,[2] and Soler and Brull.[3] Recently, Bahar and Hetnarski[4] extended their transfer matrix approach to deal with the coupled thermoelasticity of a layered medium. Additionally, Takeuti and Tsuju[5] considered the coupling effect when they analyzed the thermoelasticity problem of a plate heated by linear heat sources on both surfaces. They found that considering the coupling terms results in a delay in the progress of temperature distribution, a decrease in the value of the maximum temperature, and a narrower shape of the curve compared with neglecting the coupling effect. Further, there was a 9% increase in the thermal stresses for the case studied and a delay in the progress of the thermal stress distribution and the position of its maximum value with an increase in time. Other relevant recent studies include Takeuti and Furkawa[6] and Takeuti and Tanigawa.[7] The finite-element method was first applied to a coupled thermoelasticity problem by Chen and Ghoneim.[8] Results obtained[9] indicate that, under a high rate of loading, the coupling term should not be ignored as it could cause temperature fluctuations of the order of 5 to 10%.

The present Technical Note focuses on the effect of the thermomechanical coupling on the thermal response of an isotropic beam subjected to a nonuniform temperature. An analytical technique based on an eigenfunction method has been used to obtain the stress and the temperature distributions using the coupled thermoelasticity theory. Different comparisons have been made between the present solutions and those obtained by the classical uncoupled quasistatic thermoelasticity theory.

Analysis

Using energy principles, one can obtain the following equation for an elastic linear solid subjected to a temperature change:

$$K_{ij}T_{,ij} + \rho r = \rho c_e \dot{T} + T_0 c_{ijk1}\alpha_{k1}\dot{\epsilon}_{ij} \tag{1}$$

where ρ, c_e, T_0, r, c_{ijkl}, and α_{kl} are mass density, specific heat, reference temperature, heat supply per unit mass, the compliance tensor, and the expansion coefficient vector, and K_{ij}, T, and $\dot{\epsilon}_{ij}$ are the thermal conductivity tensor, the temperature, and the strain-rate tensor respectively. For isotropic materials, Eq. (1) takes the familiar form

$$kT_{,ii} + \rho r = \rho c_e \dot{T} + \alpha(3\lambda + 2\mu)T_0\dot{\epsilon}_{ij} \tag{2}$$

The appearance of the mechanical coupling term in the general thermoelastic problem can be interpreted as if an external action produces some variation of strains within the structural element. The equation shows that these strains are accompanied by variations in temperature and consequently by a flow of heat. Similarly, if the structure is subjected to a nonuniform temperature, the coupling term indicates that the way the structural element deforms due to this thermal exposure affects the temperature distribution.

Equation (2) and the following equilibrium equation compose the two governing differential equations for any thermal elastic problem

$$\sigma_{ij,j} + f_i = \rho\ddot{u}_i, \tag{3}$$

Where σ_{ij}, f, and u are the stress tensor, the body force, and the displacement respectively. If the coupled quasistatic theory is used to solve the thermal-elastic problem, the deformations (or stresses) and temperature distributions are determined simultaneously by solving Eqs. (2) and (3). When the coupling term [the last term in Eq. (2)] is neglected, the problem separates into two distinct equations to be solved consecutively: the first (heat conduction problem) to determine the temperature distribution, and the second (elasticity problem) to determine the deformations.

Now, consider a beam bounded by the planes $y = h$ and $y = +h$. The surface $y = -h$ is insulated, and the surface $y = +h$ is exposed to a constant heat input q for $t > 0$. The following assumptions are made.

1) The material of the beam is isotropic and obeys the restrictions of linear elasticity theory.

2) Mechanical and thermal properties remain unchanged with respect to temperature and time.

3) The plane-stress assumption holds; $\sigma_{zi} = 0$, $i = x, y$, and z.

4) For $L >> b$, $2h$, the semi-inverse assumption holds, i.e., $T = T(y)$, $\sqrt{xx} = \sigma_{xx}(y)$, and $\sigma_{yy} = \sigma_{xy} = 0$.

5) The dynamic effect on the thermal response is neglected (i.e., the inertia term in the equilibrium equation).

Received March 31, 1989; revision received Aug. 14, 1989.

*Graduate Student, Department of Civil Engineering.

†Professor and Chairman, Department of Civil Engineering. Associate Fellow AIAA.